Acta Mech
https://doi.org/10.1007/s00707-017-2033-y

ORIGINAL PAPER

Vlado A. Lubarda

On elastic fields of perfectly bonded and sliding circular inhomogeneities in an infinite matrix

Received: 4 July 2017 / Revised: 18 August 2017

Abstract The solutions to classical problems of perfectly bonded and sliding circular inhomogeneities in a remotely loaded infinite matrix are constructed by using an appealing choice of dimensionless material parameters that represent the in-plane average normal stress and the maximum shear stress at the center of the inhomogeneity, scaled by the corresponding measures of remote stress. The ovalization of the inhomogeneity and the effects of material parameters on stress concentration are discussed. The range of material parameters is specified for which the inhomogeneity with a perfectly bonded interface can expand in vertical direction under horizontal remote loading. For some combination of material properties, the maximum compressive hoop stress in the matrix along the interface can be larger than the maximum hoop stress around a circular void under tensile remote loading. The strain energies stored in perfectly bonded and sliding inhomogeneities are evaluated and discussed.

1 Introduction

The stress and displacement fields within and outside of a circular inhomogeneity in an infinitely extended matrix under remote uniform loading are well known [1]. They are of fundamental importance for the mechanics of heterogeneous media and for the study of the mechanical behavior of composite materials [2,3]. If the inhomogeneity is a void, the problem reduces to a famous Kirsch problem [4,5], which is of fundamental importance for the study of stress concentration, plastic deformation, and material failure under tensile and compressive loadings [6–8]. Both perfectly bonded and sliding interfaces were considered, as well as imperfect interfaces which cannot support shear and tensile traction [9,10], or imperfect interfaces with a prescribed relationship between the interface traction and displacement [11,12]. Various approaches were employed in the derivation of elastic fields, most of which are based on the use of functions of complex variables [1,13], or the use of the Airy stress function or the Papkovich–Neuber displacement potentials [14–19]. Sliding circular inclusions in an elastic half-space were considered in [20]. A number of papers was also devoted to elliptical inhomogeneities and inclusions [21–26], after a seminal paper on ellipsoidal inclusions by Eshelby [27].

We present in this paper an appealing derivation of a solution to perfectly bonded and a sliding inhomogeneity in a remotely loaded infinite matrix by introducing and employing a new set of material parameters, which have simple physical interpretation in terms of stresses at the center of the inhomogeneity. In the case of a perfectly bonded interface, we begin the analysis in the spirit of a semi-inverse method of elasticity by making the assumption that under a uniform remote loading of the matrix the circular inhomogeneity deforms into an elliptical shape. Such deformation necessarily implies that the inhomogeneity is in the state of uniform strain and stress, because only the displacement field linear in the Cartesian coordinates x and y transforms a

V. A. Lubarda (✉)
Department of NanoEngineering, University of California, San Diego, La Jolla, CA 92093-0448, USA
E-mail: vlubarda@ucsd.edu

Published online: 22 December 2017

circle into an ellipse.[1] Furthermore, the symmetry requires that the material line elements along the x and y directions, emanating from the center of a circular inhomogeneity (Fig. 1), remain along these directions upon the application of remote loading in the horizontal direction (p), or remote biaxial loading (p, q). This means that the shear strain $\epsilon^{\rm i}_{xy}$ and thus the shear stress $\sigma^{\rm i}_{xy}$ both vanish within the inhomogeneity, so that its state of stress is a uniform biaxial state of stress $(\sigma^{\rm i}_{xx}, \sigma^{\rm i}_{yy})$. We then show that the average in-plane normal stress and the maximum in-plane shear stress in the inhomogeneity, $\sigma^{\rm i} = (\sigma^{\rm i}_{xx} + \sigma^{\rm i}_{yy})/2$ and $\tau^{\rm i} = (\sigma^{\rm i}_{xx} - \sigma^{\rm i}_{yy})/2$, normalized by the corresponding measures of remote stress $(p+q)/2$ and $(p-q)/2$, specify the dimensionless material parameters

$$\bar{\sigma}^{\rm i} = \frac{2\sigma^{\rm i}}{p+q} = \frac{1+\kappa_1}{2+\Gamma(\kappa_2-1)}, \quad \bar{\tau}^{\rm i} = \frac{2\tau^{\rm i}}{p-q} = \frac{1+\kappa_1}{\Gamma+\kappa_1}, \tag{1.1}$$

which appear in all expressions for the stress and displacement fields in the matrix and the inhomogeneity. The ratio of the shear moduli of the matrix to the inhomogeneity is $\Gamma = \mu_1/\mu_2$, and κ_1 and κ_2 are the corresponding Kolosov's constants, dependent on Poisson's ratios of two materials. It is noted that a reciprocal definition $(\Gamma = \mu_2/\mu_1)$ has been more frequently used in the literature, which implies a void when $\Gamma = 0$, but we adopted the definition $\Gamma = \mu_1/\mu_2$ because it has led to a somewhat more compact representation of the expressions for the normalized average normal stress and the maximum shear stress at the center of the inhomogeneity.

In the case of an inhomogeneity with a sliding interface, incapable of supporting shear traction, the radial traction is given by the same expression as in the case of a perfectly bonded interface, $t_r = \sigma^{\rm i}_o + \tau^{\rm i}_o \cos 2\theta$, except that $\sigma^{\rm i}_o$ and $\tau^{\rm i}_o$ now represent the average normal stress and the maximum shear stress at the center of the inhomogeneity. In the absence of the interface shear traction, the inhomogeneity is deformed into an oval rather than an elliptical shape, and is, therefore, nonuniformly stressed and strained. The dimensionless material parameters which define the elastic fields in the matrix and the inhomogeneity are in this case

$$\bar{\sigma}^{\rm i}_o = \frac{2\sigma^{\rm i}_o}{p+q} = \bar{\sigma}^{\rm i} = \frac{1+\kappa_1}{2+\Gamma(\kappa_2-1)}, \quad \bar{\tau}^{\rm i}_o = \frac{2\tau^{\rm i}_o}{p-q} = \frac{6(1+\kappa_1)}{1+3\kappa_1+\Gamma(3+\kappa_2)}. \tag{1.2}$$

In terms of these parameters, we discuss the features of the mechanical response related to the ovalization of bonded and sliding inhomogeneities and the stress concentration around their interface with the matrix.

2 Circular inhomogeneity in an infinitely extended stretched matrix

Figure 1 shows a perfectly bonded circular inhomogeneity of radius a in an infinitely extended matrix under uniform remote stress $\sigma^0_{xx} = p$. The elastic properties of the isotropic matrix are (μ_1, ν_1), and those of the isotropic inhomogeneity are (μ_2, ν_2), where μ is the shear modulus, and ν is Poisson's ratio. The objective is to find the stress and displacement fields in the inhomogeneity and the matrix, for both plane strain and plain stress conditions. In the spirit of a semi-inverse method of elasticity, we assume that a circular inhomogeneity will deform into an elliptical shape. Since only a linear mapping (displacement components given by linear functions of x and y) transforms a circle into an ellipse, the state of strain and thus stress in the inhomogeneity is uniform. The symmetry requires that the shear stress $\sigma^{\rm i}_{xy}$ vanishes, so that the state of stress within the inhomogeneity is a uniform biaxial state of stress $(\sigma^{\rm i}_{xx}, \sigma^{\rm i}_{yy})$. To determine these stresses, we consider in Figs. 2 and 3 the free-body diagrams of the inhomogeneity and the matrix alone. In Fig. 2, the boundary $r = a$ of the inhomogeneity is under the interface traction components

$$t^*_r = \sigma^{\rm i} + \tau^{\rm i} \cos 2\theta, \quad t^*_\theta = -\tau^{\rm i} \sin 2\theta \tag{2.1}$$

where

$$\sigma^{\rm i} = \frac{1}{2}(\sigma^{\rm i}_{xx} + \sigma^{\rm i}_{yy}), \quad \tau^{\rm i} = \frac{1}{2}(\sigma^{\rm i}_{xx} - \sigma^{\rm i}_{yy}) \tag{2.2}$$

are the in-plane average normal stress and the maximum shear stress in the inhomogeneity. It will be shown in the paper that the normalized version of these stresses, $\bar{\sigma}_{\rm i} = 2\sigma^{\rm i}/p$ and $\bar{\tau}_{\rm i} = 2\tau^{\rm i}/p$, represent the material

[1] This uniformity of stress within the inhomogeneity was proven in a more general context of three-dimensional ellipsoidal inhomogeneities by Eshelby [27], whose work played a prominent role in the development of micromechanics and mechanics of composites [2,3,28–30].

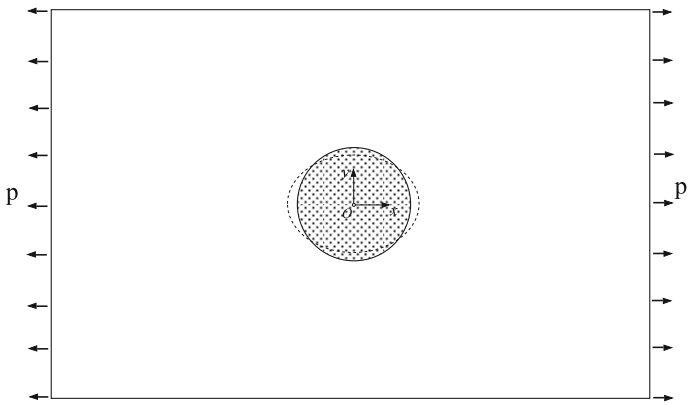

Fig. 1 A circular inhomogeneity within an infinitely extended matrix under a remote uniform stress p. In the case of a perfectly bonded interface, a circular inhomogeneity deforms into an elliptical shape and is thus uniformly strained and stressed

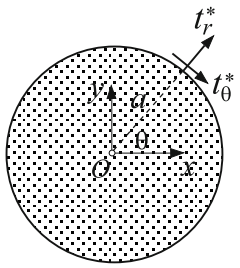

Fig. 2 A free-body diagram of a circular inhomogeneity of radius a taken out of the matrix. The interface traction components over the boundary $r = a$ are t_r^* and t_θ^*, given by (2.1)

parameters of the problem that play a prominent role and naturally appear in all expressions for the stress and displacement fields in the matrix and the inhomogeneity. The uniform state of stress within the inhomogeneity, expressed in polar coordinates, is

$$\sigma_{rr}^{\mathrm{i}} = \sigma^{\mathrm{i}} + \tau^{\mathrm{i}} \cos 2\theta, \quad \sigma_{\theta\theta}^{\mathrm{i}} = \sigma^{\mathrm{i}} - \tau^{\mathrm{i}} \cos 2\theta, \quad \sigma_{r\theta}^{\mathrm{i}} = -\tau^{\mathrm{i}} \sin 2\theta. \tag{2.3}$$

The corresponding radial and circumferential displacement components are

$$u_r^{\mathrm{i}} = \frac{r}{2\mu_2}\left(\frac{\kappa_2 - 1}{2}\sigma^{\mathrm{i}} + \tau^{\mathrm{i}} \cos 2\theta\right), \quad u_\theta^{\mathrm{i}} = -\frac{r}{2\mu_2}\tau^{\mathrm{i}} \sin 2\theta \tag{2.4}$$

where

$$\kappa = \begin{cases} 3 - 4\nu, & \text{for plane strain} \quad (1 \le \kappa \le 3), \\ (3 - \nu)/(1 + \nu), & \text{for plane stress} \quad (5/3 \le \kappa \le 3). \end{cases} \tag{2.5}$$

Figure 3 shows the free-body diagram of the matrix, with the interface traction applied to the inner circle $r = a$, and the remote tension σ at infinity. The Airy stress function for this problem can be easily constructed by superposition of two problems, a uniformly stressed matrix and the matrix loaded by properly adjusted traction over the inner surface of the hole, $\hat{t}_r = \hat{\sigma} + \hat{\tau} \cos 2\theta$ and $\hat{t}_\theta = -\hat{\tau} \sin 2\theta$, where

$$\hat{\sigma} = \sigma^{\mathrm{i}} - \frac{p}{2}, \quad \hat{\tau} = \tau^{\mathrm{i}} - \frac{p}{2}. \tag{2.6}$$

This gives

$$\Phi^{\mathrm{m}} = \frac{p}{4}(1 - \cos 2\theta) + \hat{\sigma} a^2 \ln \frac{r}{a} - \hat{\tau} a^2 \left(1 - \frac{1}{2}\frac{a^2}{r^2}\right) \cos 2\theta. \tag{2.7}$$

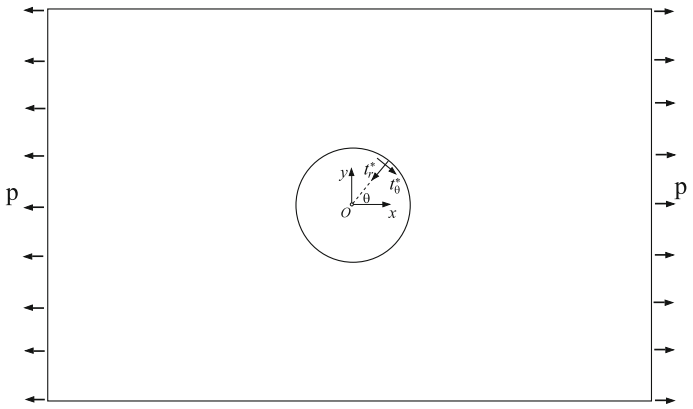

Fig. 3 A free-body diagram of a remotely loaded matrix with the inhomogeneity taken out and replaced by the interface tractions t_r^* and t_θ^* over the boundary of the inner circle $r = a$, which are opposite to those shown in Fig. 2

The stresses in the matrix are then

$$\begin{aligned}
\sigma_{rr}^{\rm m} &= \frac{p}{2} + \hat{\sigma}\,\frac{a^2}{r^2} + \left[\frac{p}{2} + \hat{\tau}\left(4\,\frac{a^2}{r^2} - 3\,\frac{a^4}{r^4}\right)\right]\cos 2\theta,\\
\sigma_{\theta\theta}^{\rm m} &= \frac{p}{2} - \hat{\sigma}\,\frac{a^2}{r^2} - \left(\frac{p}{2} - 3\hat{\tau}\,\frac{a^4}{r^4}\right)\cos 2\theta,\\
\sigma_{r\theta}^{\rm m} &= \left[-\frac{p}{2} + \hat{\tau}\left(2\,\frac{a^2}{r^2} - 3\,\frac{a^4}{r^4}\right)\right]\sin 2\theta.
\end{aligned} \tag{2.8}$$

The corresponding displacement components are obtained by integration from strains,

$$\epsilon_{\alpha\beta}^{\rm m} = \frac{1}{2\mu_1}\left[\sigma_{\alpha\beta}^{\rm m} - \frac{3-\kappa_1}{4}\left(\sigma_{rr}^{\rm m} + \sigma_{\theta\theta}^{\rm m}\right)\delta_{\alpha\beta}\right], \quad (\alpha, \beta = r, \theta), \tag{2.9}$$

where $\delta_{\alpha\beta}$ stands for the Kronecker delta. This gives

$$\begin{aligned}
2\mu_1 u_r^{\rm m} &= \frac{pr}{4}\,(\kappa_1 - 1) - \hat{\sigma}\,\frac{a^2}{r} + \left[\frac{pr}{2} - \hat{\tau}\left((1+\kappa_1)\,\frac{a^2}{r} - \frac{a^4}{r^3}\right)\right]\cos 2\theta,\\
2\mu_1 u_\theta^{\rm m} &= -\left[\frac{pr}{2} - \hat{\tau}\left((\kappa_1 - 1)\frac{a^2}{r} + \frac{a^4}{r^3}\right)\right]\sin 2\theta.
\end{aligned} \tag{2.10}$$

2.1 Interface continuity conditions

The continuity conditions along the perfectly bonded interface are

$$u_r^{\rm i}(a,\theta) = u_r^{\rm m}(a,\theta), \quad u_\theta^{\rm i}(a,\theta) = u_\theta^{\rm m}(a,\theta) \tag{2.11}$$

where, from expressions (2.4) and (2.10),

$$u_r^{\rm i}(a,\theta) = \frac{a}{2\mu_2}\left(\frac{\kappa_2 - 1}{2}\,\sigma^{\rm i} + \tau^{\rm i}\cos 2\theta\right), \quad u_\theta^{\rm i} = -\frac{a}{2\mu_2}\,\tau^{\rm i}\sin 2\theta, \tag{2.12}$$

and

$$\begin{aligned}
u_r^{\rm m}(a,\theta) &= \frac{a}{2\mu_1}\left[\frac{p}{4}\,(1+\kappa_1) - \sigma^{\rm i} + \left(\frac{p}{2}\,(1+\kappa_1) - \kappa_1\tau^{\rm i}\right)\cos 2\theta\right],\\
u_\theta^{\rm m}(a,\theta) &= -\frac{a}{2\mu_1}\left[\frac{p}{2}\,(1+\kappa_1) - \kappa_1\tau^{\rm i}\right]\sin 2\theta.
\end{aligned} \tag{2.13}$$

The continuity conditions (2.11) then give

$$\sigma^{\mathrm{i}} = \frac{p(1+\kappa_1)}{2[2+\Gamma(\kappa_2-1)]}, \quad \tau^{\mathrm{i}} = \frac{p(1+\kappa_1)}{2(\Gamma+\kappa_1)}, \quad (\Gamma = \mu_1/\mu_2). \tag{2.14}$$

Thus, we identify the dimensionless (necessarily positive) material parameters

$$\bar{\sigma}^{\mathrm{i}} = \frac{2\sigma^{\mathrm{i}}}{p} = \frac{1+\kappa_1}{2+\Gamma(\kappa_2-1)}, \quad \bar{\tau}^{\mathrm{i}} = \frac{2\tau^{\mathrm{i}}}{p} = \frac{1+\kappa_1}{\Gamma+\kappa_1}, \tag{2.15}$$

which represent the in-plane average normal stress and the maximum shear stress in the inhomogeneity, scaled by the corresponding measures of the remotely applied stress.

2.2 Final expressions for the stress and displacement fields

By using (2.14) and (2.6), the normalized stress components in the matrix (2.8) can be expressed as

$$\begin{aligned}
2\,\frac{\sigma^{\mathrm{m}}_{rr}}{p} &= 1 + (\bar{\sigma}^{\mathrm{i}}-1)\frac{a^2}{r^2} + \left[1 + (\bar{\tau}^{\mathrm{i}}-1)\left(4\,\frac{a^2}{r^2} - 3\,\frac{a^4}{r^4}\right)\right]\cos 2\theta,\\
2\,\frac{\sigma^{\mathrm{m}}_{\theta\theta}}{p} &= 1 - (\bar{\sigma}^{\mathrm{i}}-1)\frac{a^2}{r^2} - \left[1 - 3(\bar{\tau}^{\mathrm{i}}-1)\frac{a^4}{r^4}\right]\cos 2\theta,\\
2\,\frac{\sigma^{\mathrm{m}}_{r\theta}}{p} &= -\left[1 - (\bar{\tau}^{\mathrm{i}}-1)\left(2\,\frac{a^2}{r^2} - 3\,\frac{a^4}{r^4}\right)\right]\sin 2\theta.
\end{aligned} \tag{2.16}$$

Honein and Herrmann [13] derived the equivalent expressions to (2.15) by using their heterogenization procedure within the formalism of the functions of complex variables, reproducing the results previously reported by Muskhelishvili [1]. Their coefficients γ and β are related to $\bar{\sigma}^{\mathrm{i}}$ and $\bar{\tau}^{\mathrm{i}}$ by $\gamma = 1 - \bar{\sigma}^{\mathrm{i}}$ and $\beta = 1 - \bar{\tau}^{\mathrm{i}}$, so that, in (2.6), $\hat{\sigma} = -\gamma p/2$ and $\hat{\tau} = -\beta p/2$. Other combinations of material parameters have also been used [15]. If the inhomogeneity is a void ($\Gamma = \infty$), then $\bar{\sigma}^{\mathrm{i}} = \bar{\tau}^{\mathrm{i}} = 0$, and relations (2.15) reduce to well-known Kirsch expressions [5,6].

The normalized displacement components in the matrix are

$$\begin{aligned}
\frac{u^{\mathrm{m}}_r}{u^{\mathrm{m}}} &= \frac{\kappa_1-1}{2}\,\frac{r}{a} - (\bar{\sigma}^{\mathrm{i}}-1)\,\frac{a}{r} + \left[\frac{r}{a} - (\bar{\tau}^{\mathrm{i}}-1)\left((1+\kappa_1)\,\frac{a}{r} - \frac{a^3}{r^3}\right)\right]\cos 2\theta,\\
\frac{u^{\mathrm{m}}_\theta}{u^{\mathrm{m}}} &= -\left[\frac{r}{a} - (\bar{\tau}^{\mathrm{i}}-1)\left((\kappa_1-1)\frac{a}{r} + \frac{a^3}{r^3}\right)\right]\sin 2\theta
\end{aligned} \tag{2.17}$$

where the normalizing displacement factor is $u^{\mathrm{m}} = (pa)/(4\mu_1)$.

The polar components of normalized stresses within the inhomogeneity are

$$2\,\frac{\sigma^{\mathrm{i}}_{rr}}{p} = \bar{\sigma}^{\mathrm{i}} + \bar{\tau}^{\mathrm{i}}\cos 2\theta, \quad 2\,\frac{\sigma^{\mathrm{i}}_{\theta\theta}}{p} = \bar{\sigma}^{\mathrm{i}} - \bar{\tau}^{\mathrm{i}}\cos 2\theta, \quad 2\,\frac{\sigma^{\mathrm{i}}_{r\theta}}{p} = -\bar{\tau}^{\mathrm{i}}\sin 2\theta, \tag{2.18}$$

with the corresponding Cartesian components

$$\sigma^{\mathrm{i}}_{xx} = \frac{1}{2}\,(\bar{\sigma}^{\mathrm{i}} + \bar{\tau}^{\mathrm{i}})p, \quad \sigma^{\mathrm{i}}_{yy} = \frac{1}{2}\,(\bar{\sigma}^{\mathrm{i}} - \bar{\tau}^{\mathrm{i}})p. \tag{2.19}$$

Since $\bar{\sigma}^{\mathrm{i}}$ and $\bar{\tau}^{\mathrm{i}}$ are both positive, σ^{i}_{xx} is necessarily positive for $p > 0$, while σ^{i}_{yy} can be either positive or negative (tensile or compressive), depending whether $\bar{\sigma}^{\mathrm{i}}$ is larger or smaller than $\bar{\tau}^{\mathrm{i}}$. If $\kappa_1 = \kappa_2 = 2$ (which happens in plane strain for $\nu_1 = \nu_2 = 1/4$, and in plane stress for $\nu_1 = \nu_2 = 1/3$), then $\bar{\sigma}^{\mathrm{i}} = \bar{\tau}^{\mathrm{i}} = 3(2+\Gamma)^{-1}$ for any value of the shear modulus ratio $\Gamma = \mu_1/\mu_2$, and in this case $\sigma^{\mathrm{i}}_{yy} \equiv 0$.

2.3 Ovalization

The normalized radial and circumferential displacement components within the inhomogeneity are

$$\frac{u_r^{\rm i}}{u^{\rm i}} = \left(\frac{\kappa_2 - 1}{2}\,\bar{\sigma}^{\rm i} + \bar{\tau}^{\rm i}\cos 2\theta\right)\frac{r}{a}, \quad \frac{u_\theta^{\rm i}}{u^{\rm i}} = -\left(\bar{\tau}^{\rm i}\sin 2\theta\right)\frac{r}{a} \tag{2.20}$$

where $u^{\rm i} = (pa)/(4\mu_2)$. The corresponding Cartesian components are

$$\frac{u_x^{\rm i}}{u^{\rm i}} = \left(\frac{\kappa_2 - 1}{2}\,\bar{\sigma}^{\rm i} + \bar{\tau}^{\rm i}\right)\frac{x}{a}, \quad \frac{u_y^{\rm i}}{u^{\rm i}} = \left(\frac{\kappa_2 - 1}{2}\,\bar{\sigma}^{\rm i} - \bar{\tau}^{\rm i}\right)\frac{y}{a}. \tag{2.21}$$

The horizontal diameter of the inhomogeneity is always increased by the application of stress $p > 0$ (unless the inhomogeneity is rigid), while its vertical diameter can increase or decrease, depending on the combination of material properties. It can be readily verified that $\epsilon_{yy}^{\rm i} > 0$ if $(\kappa_1 - \Gamma)(\kappa_2 - 1) > 4$, but this inequality is satisfied only in some extreme cases of low values of Γ and high values of κ_1 and κ_2 (i.e., low values of Poisson's ratios ν_1 and ν_2). For example, if $\kappa_1 = \kappa_2 = 2.6$, the vertical diameter of the inhomogeneity will slightly increase ($\epsilon_{yy}^{\rm i} > 0$) if $0 < \Gamma < 0.1$. Figure 4 shows the deformed elliptical shape of the inhomogeneity for $\Gamma = 0.1$ in two cases: $\kappa_1 = \kappa_2 = 2$ (vertical diameter decreases), and $\kappa_1 = \kappa_2 = 2.8$ (vertical diameter increases).

In the case of void, its horizontal diameter increases by $2u_x^{\rm i}(a) = 3(1 + \kappa_1)(pa)/(4\mu_1)$, while its vertical diameter decreases by $(1/3)$ of that amount. This can be compared with the case of identical properties of the inhomogeneity and the matrix, when the horizontal diameter of the circle of radius a increases by $(\kappa_1 + 1)(pa)/(4\mu_1)$, while its vertical diameter decreases by $(3 - \kappa_1)(pa)/(4\mu_1)$. In general, the ovalization of a circular inhomogeneity, i.e., its degree of the ellipsoidalization (e), can be defined as

$$e = \frac{1 + \epsilon_{yy}^{\rm i}}{1 + \epsilon_{xx}^{\rm i}} \approx 1 + \epsilon_{yy}^{\rm i} - \epsilon_{xx}^{\rm i} = 1 - \frac{p}{2\mu_2}\,\bar{\tau}^{\rm i}, \tag{2.22}$$

which is, as expected, independent of the parameter $\bar{\sigma}^{\rm i}$, associated with the average in-plane normal stress in the inhomogeneity.

By calculating the work of the interface tractions on the corresponding displacements, the strain energy (per unit thickness) stored in the inhomogeneity is

$$E_{\rm B}^{\rm i} = \frac{p^2 a^2 \pi}{16\mu_2}\left[(\kappa_2 - 1)(\bar{\sigma}^{\rm i})^2 + 2(\bar{\tau}^{\rm i})^2\right]. \tag{2.23}$$

The plot of $E_{\rm B}^{\rm i}$ versus Γ is shown in Fig. 7 for several values of parameters κ_1 and κ_2. The plot also shows the variation of the strain energy $E_{\rm S}^{\rm i}$ corresponding to an inhomogeneity with a sliding interface, considered in Sect. 3.

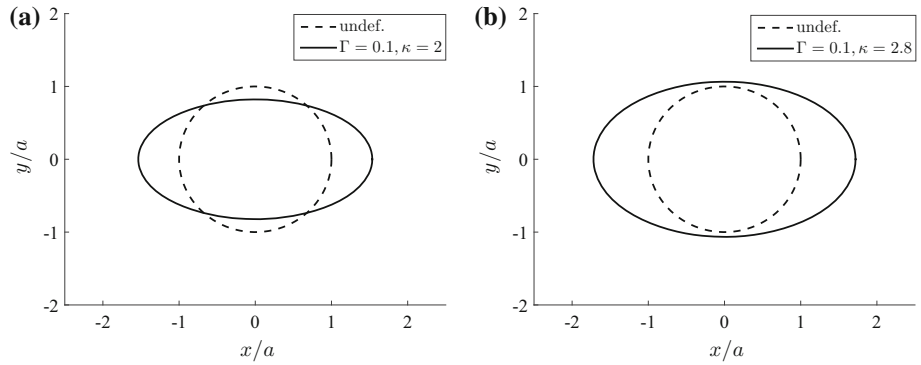

Fig. 4 The deformed elliptical shape of an originally circular inhomogeneity with $\Gamma = 0.1$ in the case: **a** $\kappa_1 = \kappa_2 = 2$ (vertical diameter decreases), and **b** $\kappa_1 = \kappa_2 = 2.8$ (vertical diameter increases). The shown displacements are magnified by the ratio μ_2/p

2.4 Stress concentration

The hoop stress along the interface on the matrix side is

$$\sigma^{\rm m}_{\theta\theta}(a,\theta)=\frac{p}{2}\left[2-\bar{\sigma}^{\rm i}-(4-3\bar{\tau}^{\rm i})\cos 2\theta\right]. \tag{2.24}$$

In view of (2.24) and (2.19), the discontinuity of the hoop stress along the interface is

$$\left(\sigma^{\rm m}_{\theta\theta}-\sigma^{\rm i}_{\theta\theta}\right)_{r=a}=p\left[1-\bar{\sigma}^{\rm i}-2(1-\bar{\tau}^{\rm i})\cos 2\theta\right]. \tag{2.25}$$

The stress concentration factor at $\theta=\pi/2$ is

$$\frac{\sigma^{\rm m}_{\theta\theta}(a,\pi/2)}{p}=3-\frac{1}{2}\,(\bar{\sigma}^{\rm i}+3\bar{\tau}^{\rm i}), \tag{2.26}$$

which is always lower than the stress concentration factor of 3 corresponding to a circular hole. However,

$$\frac{\sigma^{\rm m}_{\theta\theta}(a,0)}{p}=-1-\frac{1}{2}\,\left(\bar{\sigma}^{\rm i}-3\bar{\tau}^{\rm i}\right) \tag{2.27}$$

can be either larger or smaller than the value of -1 corresponding to a circular hole. It is smaller than -1 if $\bar{\sigma}^{\rm i}>3\bar{\tau}^{\rm i}$, which can be satisfied only in the case of plane strain, provided that

$$\Gamma>\frac{6-\kappa_1}{4-3\kappa_2},\quad \kappa_2<4/3. \tag{2.28}$$

For example, if $\kappa_1=2,\kappa_2=7/6$, and $\Gamma=20$, it follows that $\sigma^{\rm m}_{\theta\theta}(a,0)=-1.077p$. As in the Kirsch problem, of particular interest are the normal stress $\sigma^{\rm m}_{xx}(0,y)$ along the y-axis and $\sigma^{\rm m}_{yy}(x,0)$ along the x-axis, which are

$$\begin{aligned}\sigma^{\rm m}_{yy}(x,0)&=\frac{p}{2}\left[(1-\bar{\sigma}^{\rm i})\frac{a^2}{x^2}-3(1-\bar{\tau}^{\rm i})\,\frac{a^4}{x^4}\right],\\ \sigma^{\rm m}_{xx}(0,y)&=\frac{p}{2}\left[2+(1-\bar{\sigma}^{\rm i})\frac{a^2}{y^2}+3(1-\bar{\tau}^{\rm i})\,\frac{a^4}{y^4}\right].\end{aligned} \tag{2.29}$$

The variations of $\sigma^{\rm m}_{yy}(x,0)$ and $\sigma^{\rm m}_{xx}(0,y)$ along the x and y axes are shown in Figs. 5a and 6a in the case $\kappa_1=\kappa_2=2$ and selected values of the shear modulus ratio $\Gamma=\mu_1/\mu_2$. For $\Gamma=1$, $\sigma^{\rm m}_{xx}(0,y)=p$ and $\sigma^{\rm m}_{yy}(x,0)=0$. The effect of κ_1 and κ_2 on the decrease of the stress concentration, relative to the stress concentration of 3 in the case of a circular void, can be examined similarly.

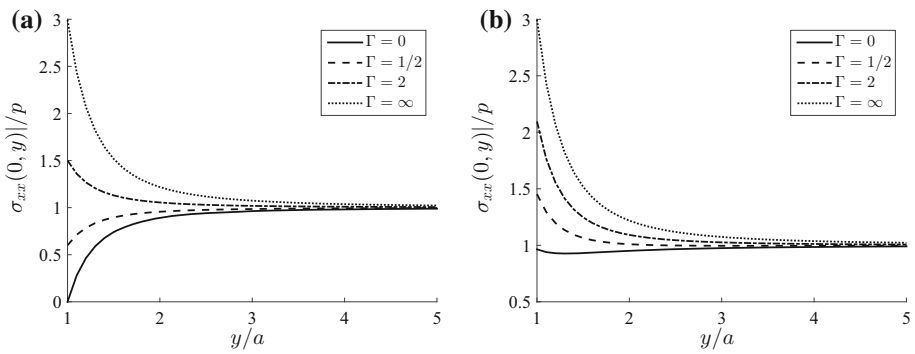

Fig. 5 The variation of $\sigma^{\rm m}_{xx}/p$ along the y-axis in the case $\kappa_1=\kappa_2=2$ and indicated values of the shear modulus ratio $\Gamma=\mu_1/\mu_2$. Part **a** is for the perfectly bonded interface, and part **b** for the sliding interface between a circular inhomogeneity and the matrix

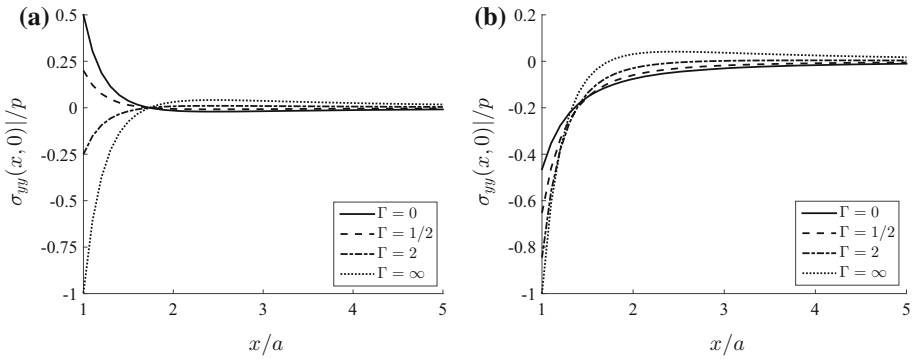

Fig. 6 **a** The variation of $\sigma^{\rm m}_{yy}/p$ along the x-axis in the case $\kappa_1 = \kappa_2 = 2$ and indicated values of the shear modulus ratio $\Gamma = \mu_1/\mu_2$. Part **a** is for the perfectly bonded interface, and part **b** for the sliding interface between a circular inhomogeneity and the matrix

3 Sliding inhomogeneity in an infinite matrix

As discussed in [15], the sliding or slipping interface may be a realistic model of a grain boundary at higher temperatures. If the interface between the inhomogeneity and the matrix in Fig. 1 cannot support the shear stress, the interface traction is in the radial direction,

$$t^*_r = \sigma^{\rm i}_o + \tau^{\rm i}_o \cos 2\theta, \quad t^*_\theta = 0. \tag{3.1}$$

The simplest $\cos 2\theta$ angle dependence, symmetric about the horizontal and vertical diameter of the inhomogeneity, as in the case of a perfectly bonded interface, was assumed, which will be confirmed by the solution. However, due to the absence of shear stress along the interface, the inhomogeneity is under an inhomogeneous state of stress. The parameters $\sigma^{\rm i}_o$ and $\tau^{\rm i}_o$ represent the in-plane average normal stress and the maximum shear stress at the center of the inhomogeneity, as shown in the sequel. The Airy stress function associated with (3.1) is

$$\Phi^{\rm i} = \frac{1}{2}\,\sigma^{\rm i}_o r^2 - \frac{1}{2}\,\tau^{\rm i}_o \left(r^2 - \frac{1}{3}\,\frac{r^4}{a^2}\right)\cos 2\theta, \tag{3.2}$$

with the corresponding stresses

$$\begin{aligned}
\sigma^{\rm i}_{rr} &= \sigma^{\rm i}_o + \tau^{\rm i}_o \cos 2\theta,\\
\sigma^{\rm i}_{\theta\theta} &= \sigma^{\rm i}_o - \tau^{\rm i}_o \left(1 - 2\,\frac{r^2}{a^2}\right)\cos 2\theta,\\
\sigma^{\rm i}_{r\theta} &= -\,\tau^{\rm i}_o \left(1 - \frac{r^2}{a^2}\right)\sin 2\theta.
\end{aligned} \tag{3.3}$$

The stress state along the circumference $r = a$ is an equal biaxial state of stress $\sigma^{\rm i}_{rr}(a,\theta) = \sigma^{\rm i}_{\theta\theta}(a,\theta) = \sigma^{\rm i}_o + \tau^{\rm i}_o \cos 2\theta$. The normalized displacement components are

$$\begin{aligned}
\frac{u^{\rm i}_r}{u^{\rm i}} &= \frac{r}{a}\left[\frac{\kappa_2 - 1}{2}\,\bar\sigma^{\rm i}_o + \bar\tau^{\rm i}_o \left(1 - \frac{3 - \kappa_2}{6}\,\frac{r^2}{a^2}\right)\cos 2\theta\right],\\
\frac{u^{\rm i}_\theta}{u^{\rm i}} &= -\,\frac{r}{a}\,\bar\tau^{\rm i}_o \left(1 - \frac{3 + \kappa_2}{6}\,\frac{r^2}{a^2}\right)\sin 2\theta
\end{aligned} \tag{3.4}$$

where $u^{\rm i} = pa/(4\mu_2)$. The normalized stress quantities are also introduced,

$$\bar\sigma^{\rm i}_o = \frac{2\sigma^{\rm i}_o}{p}, \quad \bar\tau^{\rm i}_o = \frac{2\tau^{\rm i}_o}{p}. \tag{3.5}$$

At the center of the inhomogeneity, the Cartesian stress components are

$$\sigma^{\rm i,o}_{xx} = \sigma^{\rm i}_o + \tau^{\rm i}_o, \quad \sigma^{\rm i,o}_{yy} = \sigma^{\rm i}_o - \tau^{\rm i}_o, \quad \sigma^{\rm i,o}_{xy} = 0, \tag{3.6}$$

so that

$$\sigma_o^{\mathrm{i}} = \frac{1}{2}\left(\sigma_{xx}^{\mathrm{i,o}} + \sigma_{yy}^{\mathrm{i,o}}\right), \quad \tau_o^{\mathrm{i}} = \frac{1}{2}\left(\sigma_{xx}^{\mathrm{i,o}} - \sigma_{yy}^{\mathrm{i,o}}\right), \tag{3.7}$$

confirming that σ_o^{i} and τ_o^{i} are indeed the in-plane average normal stress and the maximum shear stress at the center of the inhomogeneity, while $\bar{\sigma}_o^{\mathrm{i}}$ and $\bar{\tau}_o^{\mathrm{i}}$ represent their values normalized by $p/2$.

By the mean-value property of the harmonic function $(\sigma_{xx}^{\mathrm{i}} + \sigma_{yy}^{\mathrm{i}})$, satisfying the compatibility equation $\nabla^2(\sigma_{xx}^{\mathrm{i}} + \sigma_{yy}^{\mathrm{i}}) = 0$, it follows that σ_o^{i} is also equal to the spatial average of the in-plane mean normal stress in the inhomogeneity. The maximum in-plane shear stress within the inhomogeneity at the radius r is independent of θ and given by

$$\tau_{\max}(r) = \frac{1}{2}\left[\left(\sigma_{rr}^{\mathrm{i}} - \sigma_{\theta\theta}^{\mathrm{i}}\right)^2 + 4\left(\sigma_{r\theta}^{\mathrm{i}}\right)^2\right]^{1/2} = \tau_o^{\mathrm{i}}\left(1 - \frac{r^2}{a^2}\right). \tag{3.8}$$

Not being a harmonic function, the average value of $\tau_{\max}(r)$ is only one-half of the maximum shear stress at the center of the inhomogeneity, $\bar{\tau}_{\max} = \tau_o^{\mathrm{i}}/2$.

The Airy stress function for the matrix material is

$$\begin{aligned}\Phi^{\mathrm{m}} = {} & \frac{p}{4}\left[r^2 - 2a^2\ln\frac{r}{a} - \left(r^2 - 2a^2 + \frac{a^4}{r^2}\right)\cos 2\theta\right] \\ & + \sigma_o^{\mathrm{i}} a^2 \ln\frac{r}{a} - \frac{1}{2}\tau_o^{\mathrm{i}}\left(a^2 - \frac{1}{3}\frac{a^4}{r^2}\right)\cos 2\theta.\end{aligned} \tag{3.9}$$

The first term, proportional to $p/4$, is the part of the Airy stress function of the Kirsch problem (traction-free hole), while the remaining two terms represent the contribution from the radial traction $t_r^* = \sigma_o^{\mathrm{i}} + \tau_o^{\mathrm{i}}\cos 2\theta$ acting along the boundary of the hole. The stresses associated with (3.9) are

$$\begin{aligned}\sigma_{rr}^{\mathrm{m}} = {} & \frac{p}{2}\left[1 - \frac{a^2}{r^2} + \left(1 - 4\frac{a^2}{r^2} + 3\frac{a^4}{r^4}\right)\cos 2\theta\right] \\ & + \sigma_o^{\mathrm{i}}\frac{a^2}{r^2} + \tau_o^{\mathrm{i}}\left(2\frac{a^2}{r^2} - \frac{a^4}{r^4}\right)\cos 2\theta,\end{aligned} \tag{3.10}$$

$$\sigma_{\theta\theta}^{\mathrm{m}} = \frac{p}{2}\left[1 + \frac{a^2}{r^2} - \left(1 + 3\frac{a^4}{r^4}\right)\cos 2\theta\right] - \sigma_o^{\mathrm{i}}\frac{a^2}{r^2} + \tau_o^{\mathrm{i}}\frac{a^4}{r^4}\cos 2\theta, \tag{3.11}$$

$$\sigma_{r\theta}^{\mathrm{m}} = -\frac{p}{2}\left(1 + 2\frac{a^2}{r^2} - 3\frac{a^4}{r^4}\right)\sin 2\theta + \tau_o^{\mathrm{i}}\left(\frac{a^2}{r^2} - \frac{a^4}{r^4}\right)\sin 2\theta. \tag{3.12}$$

For convenience, the stress contributions from the Kirsch solution and from the radial traction t_r^* are shown separately. The corresponding normalized displacement components are

$$\begin{aligned}\frac{u_r^{\mathrm{m}}}{u^{\mathrm{m}}} = {} & \frac{\kappa_1 - 1}{2}\frac{r}{a} + \frac{a}{r} + \left[\frac{r}{a} + (1+\kappa_1)\frac{a}{r} - \frac{a^3}{r^3}\right]\cos 2\theta \\ & - \bar{\sigma}_o^{\mathrm{i}}\frac{a}{r} - \bar{\tau}_o^{\mathrm{i}}\left(\frac{1+\kappa_1}{2}\frac{a}{r} - \frac{1}{3}\frac{a^3}{r^3}\right)\cos 2\theta,\end{aligned} \tag{3.13}$$

$$\frac{u_\theta^{\mathrm{m}}}{u^{\mathrm{m}}} = -\left[\frac{r}{a} + (\kappa_1 - 1)\frac{a}{r} + \frac{a^3}{r^3} - \bar{\tau}_o^{\mathrm{i}}\left(\frac{1}{3}\frac{a^3}{r^3} + \frac{\kappa_1 - 1}{2}\frac{a}{r}\right)\right]\sin 2\theta \tag{3.14}$$

where $u^{\mathrm{m}} = pa/(4\mu_1)$.

The parameters $\bar{\sigma}_o^{\mathrm{i}}$ and $\bar{\tau}_o^{\mathrm{i}}$ are determined from the continuity condition for the radial displacement along the interface,

$$u_r^{\mathrm{i}}(a,\theta) = u_r^{\mathrm{m}}(a,\theta), \tag{3.15}$$

which, in view of (3.4) and (3.13), gives

$$\bar{\sigma}_o^{\mathrm{i}} = \frac{1+\kappa_1}{2 + \Gamma(\kappa_2 - 1)}, \quad \bar{\tau}_o^{\mathrm{i}} = \frac{6(1+\kappa_1)}{1 + 3\kappa_1 + \Gamma(3+\kappa_2)}. \tag{3.16}$$

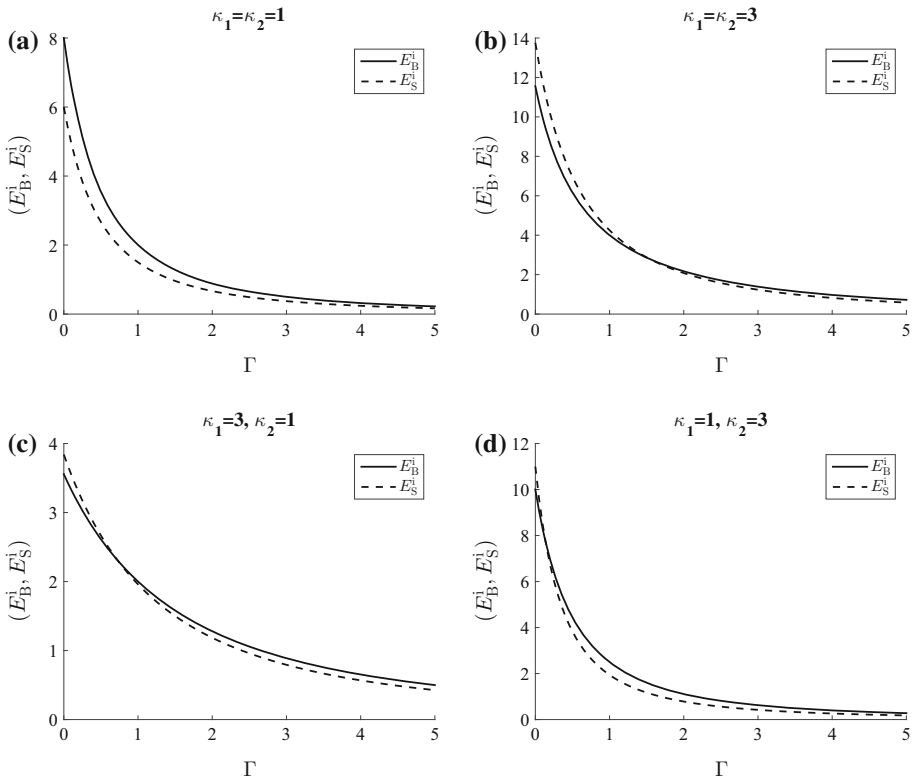

Fig. 7 The strain energy stored in a circular inhomogeneity with a perfectly bonded (solid line) and sliding interface (dashed line) versus Γ for several combinations of constants κ_1 and κ_2

The expression for $\bar{\sigma}^{\rm i}_o$ is the same as in the case of a perfectly bonded inhomogeneity, so that the average in-plane normal stress at the center of the inhomogeneity is the same in both cases. In particular, from (3.16) it follows that

$$(\bar{\sigma}^{\rm i}_o, \bar{\tau}^{\rm i}_o) = \begin{cases} 0, \quad 0, & \Gamma = \infty, \\ \dfrac{1+\kappa_1}{2}, \quad \dfrac{6(1+\kappa_1)}{1+3\kappa_1}, & \Gamma = 0, \\ \dfrac{1+\kappa_1}{1+\kappa_2}, \quad \dfrac{6(1+\kappa_1)}{4+3\kappa_1+\kappa_2}, & \Gamma = 1. \end{cases} \tag{3.17}$$

Different combinations of material parameters have been used by Dundurs [15], see equations (37) and (44) of his paper. His parameters δ and η are not directly related to a specific state of stress, but his constants D, E, and F can be expressed in terms of $\bar{\sigma}^{\rm i}_o$ and $\bar{\tau}^{\rm i}_o$ by $D = \bar{\sigma}^{\rm i}_o$, $E = -\bar{\tau}^{\rm i}_o$, and $F = \bar{\tau}^{\rm i}_o/3$.

The strain energy (per unit thickness) stored in the inhomogeneity is

$$E^{\rm i}_{\rm S} = \frac{p^2 a^2 \pi}{16\mu_2}\left[(\kappa_2 - 1)(\bar{\sigma}^{\rm i}_o)^2 + \frac{3+\kappa_2}{6}\,(\bar{\tau}^{\rm i}_o)^2\right]. \tag{3.18}$$

The plot of $E^{\rm i}_{\rm S}$ versus Γ is shown in Fig. 7 for several combinations of the bounding values of parameters κ_1 and κ_2. In the extreme case of $\kappa_1 = \kappa_2 = 1$ (i.e., $\nu_1 = \nu_2 = 0$), and the assumed plane strain conditions, the strain energy stored in the inhomogeneity with a sliding interface is always smaller than in the inhomogeneity with a bonded interface, but for other combinations of κ_1 and κ_2 this is not the case.

3.1 Stress concentration

The hoop stress within the matrix around the void is

$$\sigma^{\rm m}_{\theta\theta}(a,\theta) = \frac{p}{2}\left[2 - \bar{\sigma}^{\rm i}_o - \left(4 - \bar{\tau}^{\rm i}_o\right)\cos 2\theta\right]. \tag{3.19}$$

The discontinuity of the hoop stress across the interface is

$$\left(\sigma^{\mathrm{m}}_{\theta\theta} - \sigma^{\mathrm{i}}_{\theta\theta}\right)_{r=a} = p\left[1 - \bar{\sigma}^{\mathrm{i}}_o - 2\cos 2\theta\right]. \tag{3.20}$$

The stress concentration factor in the matrix at $\theta = \pi/2$ is

$$\frac{\sigma^{\mathrm{m}}_{\theta\theta}(a, \pi/2)}{p} = 3 - \frac{1}{2}\left(\bar{\sigma}^{\mathrm{i}}_o + \bar{\tau}^{\mathrm{i}}_o\right), \tag{3.21}$$

which is always lower than the stress concentration factor of 3 corresponding to a circular hole. However,

$$\frac{\sigma^{\mathrm{m}}_{\theta\theta}(a, 0)}{p} = -1 - \frac{1}{2}\left(\bar{\sigma}^{\mathrm{i}}_o - \bar{\tau}^{\mathrm{i}}_o\right) \tag{3.22}$$

can be either larger or smaller than the value of -1 corresponding to a circular hole. It is smaller than -1 if $\bar{\sigma}^{\mathrm{i}}_o > \bar{\tau}^{\mathrm{i}}_o$, which can be satisfied provided that

$$\Gamma > \frac{11 - 3\kappa_1}{9 - 5\kappa_2}, \quad \kappa_2 < 9/5. \tag{3.23}$$

The normal stress $\sigma^{\mathrm{m}}_{xx}(0, y)$ along the y-axis and $\sigma^{\mathrm{m}}_{yy}(x, 0)$ along the x-axis are

$$\begin{aligned}
\sigma^{\mathrm{m}}_{yy}(x, 0) &= \frac{p}{2}\left[(1 - \bar{\sigma}^{\mathrm{i}})\frac{a^2}{x^2} - \left(3 - \bar{\tau}^{\mathrm{i}}_o\right)\frac{a^4}{x^4}\right], \\
\sigma^{\mathrm{m}}_{xx}(0, y) &= \frac{p}{2}\left[2 + (1 - \bar{\sigma}^{\mathrm{i}})\frac{a^2}{y^2} + \left(3 - \bar{\tau}^{\mathrm{i}}_o\right)\frac{a^4}{y^4}\right].
\end{aligned} \tag{3.24}$$

The variations of $\sigma^{\mathrm{m}}_{yy}(0, x)$ and $\sigma^{\mathrm{m}}_{xx}(0, y)$ along the x and y axes are shown in Figs. 5b and 6b in the case $\kappa_1 = \kappa_2 = 2$ and selected values of the shear modulus ratio $\Gamma = \mu_1/\mu_2$. These plots can be compared with the corresponding plots shown in Figs. 5a and 6a for the perfectly bonded inhomogeneity. For finite values of Γ, the stress concentration at $y = a$ is larger in the case of a sliding interface. For example, for a perfectly bonded rigid inhomogeneity $\sigma^{\mathrm{m}}_{xx}(0, a) = 0$, while in the case of a sliding interface $\sigma^{\mathrm{m}}_{xx}(0, a) = 0.964\, p$ (Fig. 5a, b). Furthermore, the stress $\sigma^{\mathrm{m}}_{yy}(a, 0)$ is compressive in the case of a sliding interface for all values of Γ, while it changes from compressive to tensile as Γ decreases from ∞ to 0 in the case of a perfectly bonded interface (Fig. 6a, b).

3.2 Ovalization

The deformed shape of the inhomogeneity is specified by the displacement components along its boundary $r = a$. From (3.4), these are

$$\begin{aligned}
u^{\mathrm{i}}_r(a, \theta) &= \frac{p}{4\mu_2}\left(\frac{\kappa_2 - 1}{2}\,\bar{\sigma}^{\mathrm{i}}_o + \frac{3 + \kappa_2}{6}\,\bar{\tau}^{\mathrm{i}}_o\right) a\cos 2\theta, \\
u^{\mathrm{i}}_\theta(a, \theta) &= -\frac{p}{4\mu_2}\,\frac{3 - \kappa_2}{6}\,\bar{\tau}^{\mathrm{i}}_o\, a\sin 2\theta.
\end{aligned} \tag{3.25}$$

The ovalized shape of the deformed inhomogeneity is shown in Fig. 8 for several selected values of Γ. In each case, the parameters κ_1 and κ_2 are chosen to be equal to 2. The nonelliptical ovalization is particularly pronounced for smaller values of Γ. For comparison, the dashed lines show the elliptical deformed shape of the circular inhomogeneity with a perfectly bonded interface. For large values of Γ, the deformed shapes are almost identical for both interfaces, and identical in the limit of a void ($\Gamma \to \infty$). In each considered case, the increase in the horizontal diameter and a decrease in the vertical diameter was larger for a sliding inhomogeneity, except in the plane strain incompressible limit, when they were equal for both interfaces. There is no combination of material properties for which the vertical diameter of a sliding inhomogeneity can increase under the horizontal remote loading.

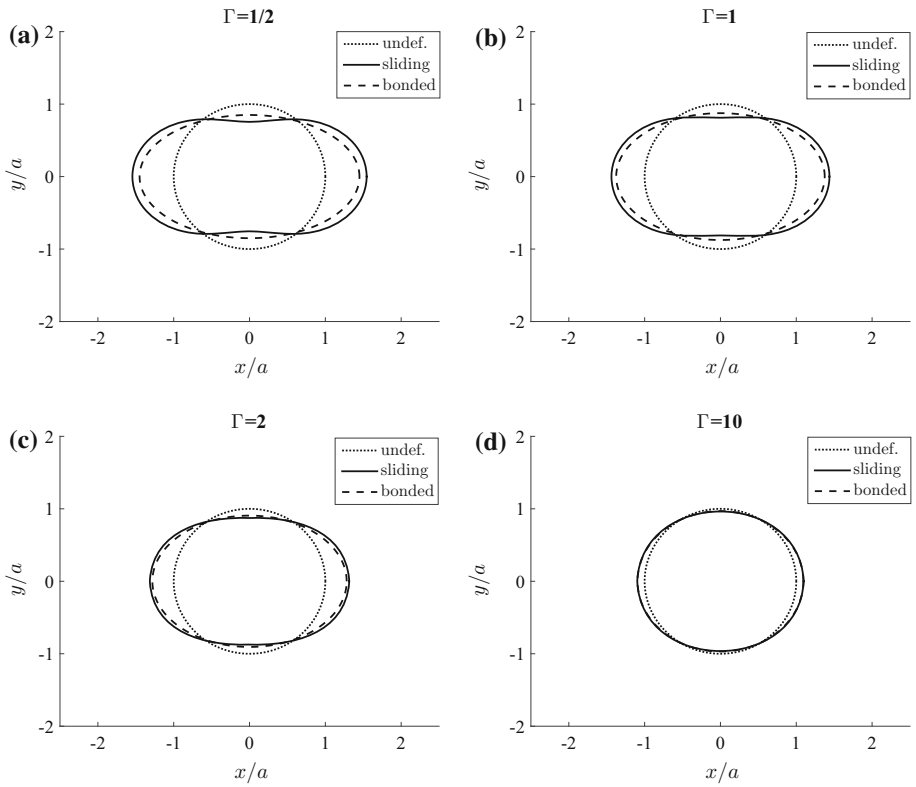

Fig. 8 The deformed shape of a circular inhomogeneity with a sliding (solid line) and perfectly bonded interface (dotted line) for several selected values of Γ and $\kappa_1 = \kappa_2 = 2$. The shown displacements are magnified by the ratio μ_2/p

4 Conclusions

The solutions to classical problems of perfectly bonded and sliding circular inhomogeneities in a remotely loaded infinite matrix are presented by using an appealing choice of dimensionless material parameters that represent the in-plane average normal stress and the maximum shear stress at the center of the inhomogeneity, scaled by the corresponding measures of remote stress. These parameters were used to evaluate and discuss the elliptical and nonelliptical ovalization of perfectly bonded and sliding inhomogeneities, and the corresponding stress concentrations around the interface. For finite values of the shear modulus ratio $\Gamma = \mu_1/\mu_2$ and considered values of the Poisson's ratios ν_1 and ν_2, the stress concentration under uniaxial loading in the case of a sliding interface is larger than in the case of a perfectly bonded interface. The hoop stress at $(a, 0)$ is compressive in the case of a sliding interface for all values of Γ, while it changes from compressive to tensile as Γ decreases in the case of a perfectly bonded interface. For some combinations of material properties, the maximum compressive hoop stress in the matrix along the interface can be larger than the maximum hoop stress around a circular void, for both perfectly bonded and sliding interfaces. The range of material parameters is specified for which a circular inhomogeneity with a perfectly bonded interface can expand in the vertical direction under horizontal remote loading, which can never occur in the case of a sliding interface. The nonelliptical ovalization of a circular inhomogeneity with sliding interface is particularly pronounced for smaller values of Γ. The strain energies stored in the bonded and sliding inhomogeneities are evaluated and discussed. In the limiting case of $\kappa_1 = \kappa_2 = 1$, under plane strain conditions, the strain energy stored in the inhomogeneity with a sliding interface is always smaller than in the inhomogeneity with a bonded interface, but for other combinations of κ_1 and κ_2 this is not the case. Stress and displacement fields for biaxial loading of bonded and sliding inhomogeneities are listed in the appendices of the paper. The obtained results may be of interest for structural design and analysis of mechanical strength and failure of heterogeneous materials under tensile and compressive loadings.

Acknowledgements This research work was supported by the Montenegrin Academy of Sciences and Arts. Discussions with Dr. Marko Lubarda and his help with numerical evaluations are gratefully acknowledged. I also thank the reviewers for their helpful comments and suggestions.

Appendix A: Biaxial loading: bonded inhomogeneity

Figure 9 shows a circular inhomogeneity in an infinitely extended matrix under remote biaxial uniform loading (p, q). The dimensionless material parameters are related to the in-plane average normal and maximum shear stress σ^{i} and τ^{i} within the inhomogeneity by

$$\bar{\sigma}^{\mathrm{i}} = \frac{1+\kappa_1}{2+\Gamma(\kappa_2-1)} = \frac{2\sigma^{\mathrm{i}}}{p+q}, \quad \bar{\tau}^{\mathrm{i}} = \frac{1+\kappa_1}{\Gamma+\kappa_1} = \frac{2\tau^{\mathrm{i}}}{p-q}.$$

In terms of these parameters, the Cartesian components of stress and displacement in the inhomogeneity are

$$\sigma^{\mathrm{i}}_{xx} = \frac{1}{2}\bar{\sigma}^{\mathrm{i}}(p+q) + \frac{1}{2}\bar{\tau}^{\mathrm{i}}(p-q), \quad \sigma^{\mathrm{i}}_{yy} = \frac{1}{2}\bar{\sigma}^{\mathrm{i}}(p+q) - \frac{1}{2}\bar{\tau}^{\mathrm{i}}(p-q),$$
$$\frac{u^{\mathrm{i}}_x}{a} = \frac{1}{4\mu_2}\left[\frac{\kappa_2-1}{2}\bar{\sigma}^{\mathrm{i}}(p+q) + \bar{\tau}^{\mathrm{i}}(p-q)\right]\frac{x}{a}, \quad \frac{u^{\mathrm{i}}_y}{a} = \frac{1}{4\mu_2}\left[\frac{\kappa_2-1}{2}\bar{\sigma}^{\mathrm{i}}(p+q) - \bar{\tau}^{\mathrm{i}}(p-q)\right]\frac{y}{a}.$$

The polar stress components in the matrix are

$$\sigma^{\mathrm{m}}_{rr} = \frac{p+q}{2}\left[1+(\bar{\sigma}^{\mathrm{i}}-1)\frac{a^2}{r^2}\right] + \frac{p-q}{2}\left[1+(\bar{\tau}^{\mathrm{i}}-1)\left(4\frac{a^2}{r^2}-3\frac{a^4}{r^4}\right)\right]\cos 2\theta,$$
$$\sigma^{\mathrm{m}}_{\theta\theta} = \frac{p+q}{2}\left[1-(\bar{\sigma}^{\mathrm{i}}-1)\frac{a^2}{r^2}\right] - \frac{p-q}{2}\left[1-3(\bar{\tau}^{\mathrm{i}}-1)\frac{a^4}{r^4}\right]\cos 2\theta,$$
$$\sigma^{\mathrm{m}}_{r\theta} = -\frac{p-q}{2}\left[1-(\bar{\tau}^{\mathrm{i}}-1)\left(2\frac{a^2}{r^2}-3\frac{a^4}{r^4}\right)\right]\sin 2\theta,$$

with the corresponding displacements

$$\frac{u^{\mathrm{m}}_r}{a} = \frac{p+q}{4\mu_1}\left[\frac{\kappa_1-1}{2}\frac{r}{a} - (\bar{\sigma}^{\mathrm{i}}-1)\frac{a}{r}\right] + \frac{p-q}{4\mu_1}\left[\frac{r}{a} - (\bar{\tau}^{\mathrm{i}}-1)\left((1+\kappa_1)\frac{a}{r} - \frac{a^3}{r^3}\right)\right]\cos 2\theta,$$
$$\frac{u^{\mathrm{m}}_\theta}{a} = -\frac{p-q}{4\mu_1}\left[\frac{r}{a} - (\bar{\tau}^{\mathrm{i}}-1)\left((\kappa_1-1)\frac{a}{r} + \frac{a^3}{r^3}\right)\right]\sin 2\theta.$$

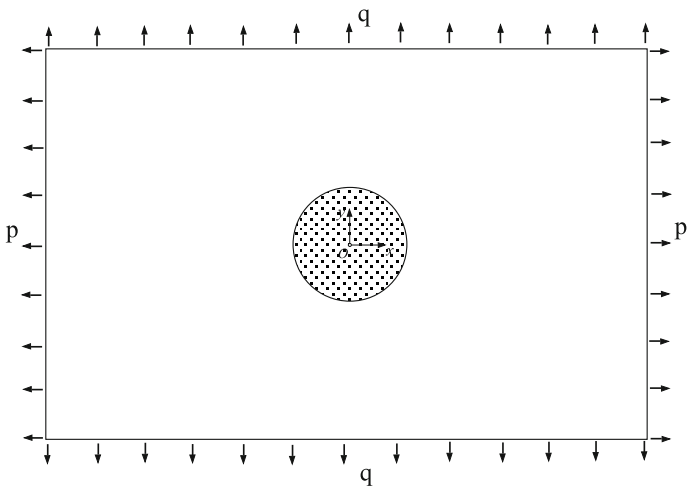

Fig. 9 A circular inhomogeneity within an infinitely extended matrix under remote uniform biaxial stress (p, q)

Appendix B: Biaxial loading: sliding inhomogeneity

If the interface of the inhomogeneity in Fig. 9 is incapable to support shear stress, the dimensionless material parameters are related to the in-plane average normal and maximum shear stress $\sigma_o^{\rm i}$ and $\tau_o^{\rm i}$ at the center of the inhomogeneity by

$$\bar{\sigma}_o^{\rm i} = \frac{2\sigma_o^{\rm i}}{p+q} = \frac{1+\kappa_1}{2+\Gamma(\kappa_2-1)}, \quad \bar{\tau}_o^{\rm i} = \frac{2\tau_o^{\rm i}}{p-q} = \frac{6(1+\kappa_1)}{1+3\kappa_1+\Gamma(3+\kappa_2)}.$$

The polar stress components within the inhomogeneity are

$$\begin{aligned}
\sigma_{rr}^{\rm i} &= \frac{p+q}{2}\,\bar{\sigma}_o^{\rm i} + \frac{p-q}{2}\,\bar{\tau}_o^{\rm i}\cos 2\theta,\\
\sigma_{\theta\theta}^{\rm i} &= \frac{p+q}{2}\,\bar{\sigma}_o^{\rm i} - \frac{p-q}{2}\bar{\tau}_o^{\rm i}\left(1-2\,\frac{r^2}{a^2}\right)\cos 2\theta,\\
\sigma_{r\theta}^{\rm i} &= -\frac{p-q}{2}\bar{\tau}_o^{\rm i}\left(1-\frac{r^2}{a^2}\right)\sin 2\theta,
\end{aligned}$$

while the normalized displacement components are

$$\begin{aligned}
\frac{u_r^{\rm i}}{a} &= \frac{p+q}{8\mu_2}\,\bar{\sigma}_o^{\rm i}(\kappa_2-1)\,\frac{r}{a} + \frac{p-q}{8\mu_2}\,\bar{\tau}_o^{\rm i}\left(2\,\frac{r}{a} - \frac{3-\kappa_2}{3}\,\frac{r^3}{a^3}\right)\cos 2\theta,\\
\frac{u_\theta^{\rm i}}{a} &= -\frac{p-q}{8\mu_2}\,\bar{\tau}_o^{\rm i}\left(2\,\frac{r}{a} - \frac{3+\kappa_2}{3}\,\frac{r^3}{a^3}\right)\sin 2\theta.
\end{aligned}$$

The polar stress components in the matrix are

$$\begin{aligned}
\sigma_{rr}^{\rm m} &= \frac{p+q}{2}\left[1+(\bar{\sigma}_o^{\rm i}-1)\frac{a^2}{r^2}\right] + \frac{p-q}{2}\left[1-(4-2\bar{\tau}_o^{\rm i})\,\frac{a^2}{r^2} + (3-\bar{\tau}^{\rm i})\,\frac{a^4}{r^4}\right]\cos 2\theta,\\
\sigma_{\theta\theta}^{\rm m} &= \frac{p+q}{2}\left[1-(\bar{\sigma}_o^{\rm i}-1)\frac{a^2}{r^2}\right] - \frac{p-q}{2}\left[1+(3-\bar{\tau}_o^{\rm i})\,\frac{a^4}{r^4}\right]\cos 2\theta,\\
\sigma_{r\theta}^{\rm m} &= -\frac{p-q}{2}\left[1-\frac{a^2}{r^2}+(3-\bar{\tau}_o^{\rm i})\left(\frac{a^2}{r^2}-\frac{a^4}{r^4}\right)\right]\sin 2\theta,
\end{aligned}$$

with the corresponding displacements

$$\begin{aligned}
\frac{u_r^{\rm m}}{a} &= \frac{p+q}{4\mu_1}\left[\frac{\kappa_1-1}{2}\,\frac{r}{a} + (1-\bar{\sigma}_o^{\rm i})\frac{a}{r}\right]\\
&\quad + \frac{p-q}{4\mu_1}\left[\frac{r}{a} + \frac{\kappa_1+1}{2}\,(2-\bar{\tau}_o^{\rm i})\frac{a}{r} - \frac{1}{3}\,(3-\bar{\tau}_o^{\rm i})\frac{a^3}{r^3}\right]\cos 2\theta,\\
\frac{u_\theta^{\rm m}}{a} &= -\frac{p-q}{4\mu_1}\left[\frac{r}{a} + \frac{\kappa_1-1}{2}\,(2-\bar{\tau}_o^{\rm i})\frac{a}{r} + \frac{1}{3}\,(3-\bar{\tau}_o^{\rm i})\frac{a^3}{r^3}\right]\sin 2\theta.
\end{aligned}$$

References

1. Muskhelishvili, N.I.: Some Basic Problems of the Mathematical Theory of Elasticity. Noordhoff, Groningen (1953)
2. Mura, T.: Micromechanics of Defects in Solids, 2nd edn. Kluwer Academic Publishers, Dordrecht (1987)
3. Nemat-Nasser, S., Hori, M.: Micromechanics: Overall Properties of Heterogeneous Materials, 2nd edn. North-Holland, Amsterdam (1999)
4. Timoshenko, S.P., Goodier, J.N.: Theory of Elasticity, 3rd edn. McGraw-Hill, New York (1970)
5. Ugural, A.C., Fenster, S.K.: Advanced Mechanics of Materials and Applied Elasticity. Prentice Hall, Upper Saddle River (2003)
6. Ghahremani, F.: Effect of grain boundary sliding on anelasticity of polycrystals. Int. J. Solids Struct. **16**, 825–845 (1980)
7. Cook, R.D., Young, W.C.: Advanced Mechanics of Materials, 2nd edn. Pearson College Division, London (1999)
8. Krajcinovic, D.: Damage Mechanics. Elsevier, Amsterdam (1996)

9. Noble, B., Hussain, M.A.: Exact solution of certain dual series for indentation and inclusion problems. Int. J. Eng. Sci. **7**, 1149–1161 (1969)
10. Keer, L.M., Dundurs, J., Kiattikomol, K.: Separation of a smooth circular inclusion from a matrix. Int. J. Eng. Sci. **1**, 1221–1233 (1973)
11. Furuhashi, R., Huang, J.H., Mura, T.: Sliding inclusions and inhomogeneities with frictional interfaces. J. Appl. Mech. **59**, 783–788 (1992)
12. Kattis, M.A., Providas, E.: Inplane deformation of a circular inhomogeneity with imperfect interface. Theor. Appl. Fract. Mech. **28**, 213–222 (1998)
13. Honein, T., Herrmann, G.: On bonded inclusions with circular or straight boundaries in plane elastostatics. J. Appl. Mech. **57**, 850–856 (1990)
14. Goodier, J.N.: Concentration of stress around spherical and cylindrical inclusions and flaws. J. Appl. Mech. **55**, 39–44 (1933)
15. Dundurs, J.: Effect of elastic constants on stress in a composite under plane deformation. J. Compos. Mater. **1**, 310–322 (1967)
16. Malvern, L.E.: Introduction to the Mechanics of Continuous Media. Prentice Hall, Upper Saddle River (1968)
17. Mura, T., Jasiuk, I., Tsuchida, E.: The stress field of a sliding inclusion. Int. J. Solids Struct. **21**, 1165–1179 (1985)
18. Lubarda, V.A.: Sliding and bonded circular inclusions in concentric cylinders. Proc. Monten. Acad. Sci. Arts **OPN 12**, 123–139 (1998)
19. Lubarda, V.A., Markenscoff, X.: Energies of circular inclusions: sliding versus bonded interfaces. Proc. R. Soc. Lond. A **455**, 961–974 (1999)
20. Lee, M., Jasiuk, I., Tsuchida, E.: The sliding circular inclusion in an elastic half-plane. J. Appl. Mech. **59**, S57–S64 (1992)
21. Stagni, L.: On the elastic field perturbation by inhomogeneities in plane elasticity. J. Appl. Math. Phys. **33**, 315–325 (1982)
22. Tsuchida, E., Mura, T., Dundurs, J.: The elastic field of an elliptic inclusion with a slipping interface. J. Appl. Mech. **53**, 103–107 (1986)
23. Jasiuk, I., Tsuchida, E., Mura, T.: The sliding inclusion under shear. Int. J. Solids Struct. **23**, 1373–1385 (1987)
24. Lubarda, V.A., Markenscoff, X.: On the stress field in sliding ellipsoidal inclusions with shear eigenstrain. J. Appl. Mech. **65**, 858–862 (1998)
25. Lubarda, V.A., Markenscoff, X.: On the absence of Eshelby property for ellipsoidal inclusions. Int. J. Solids Struct. **35**, 3405–3411 (1998)
26. Lubarda, V.A.: On the circumferential shear stress around circular and elliptical holes. Arch. Appl. Mech. **85**, 223–235 (2015)
27. Eshelby, J.D.: The determination of the elastic field of an ellipsoidal inclusion, and related problems. Proc. R. Soc. Lond. A **241**, 376–396 (1957)
28. Christensen, R.M.: Mechanics of Composite Materials. Wiley, New York (1980)
29. Voyiadjis, G.Z., Kattan, P.I.: Mechanics of Composite Materials with MATLAB. Springer, Berlin (2005)
30. Asaro, R.J., Lubarda, V.A.: Mechanics of Solids and Materials. Cambridge University Press, Cambridge (2006)